

Synthesis, characterization, crystal structure, and fabrication of photosensitive Schottky device of a binuclear Cu(II)-Salen complex: A DFT investigations.

Dhrubajyoti Majumdar ^{a*}, Bouzid Gassoumi ^b, Arka Dey ^c, Sourav Roy ^d, Sahbi Ayachi ^e,
Suman Hazra ^{a, f}, Sudipta Dalai ^{f*}

^aDepartment of Chemistry, Tamralipta Mahavidyalaya, Tamluk-721636, West Bengal, India.

^bLaboratory of Advanced Materials and Interfaces (LIMA), University of Monastir, Faculty of Sciences of Monastir, Avenue of Environment, 5000 Monastir, Tunisia.

^cDepartment of Physics, National Institute of Technology Durgapur, Durgapur 713209, India.

^d Solid State and Structural Chemistry Unit, Indian Institute of Science, Bangalore-560012, India.

^eLaboratory of Physico-Chemistry of Materials (LR01ES19), Faculty of Sciences, Avenue of the environment 5019 Monastir, University of Monastir, Tunisia.

^fDepartment of Chemistry, Vidyasagar University, Midnapore-7211102, West Bengal, India.

Corresponding author EMAIL: dmajumdar30@gmail.com, sudipta@mail.vidyasagar.ac.in

Contents of Electronic Supporting Materials

- | | |
|--|---------------------|
| 1. Optical Characterization. | Section 1.1. |
| 2. Device Fabrication. | Section 1.2. |
| 3. Optical Characterization. | Section 1.3. |
| 4. Schematic depiction of an electrical conductivity-based photo-sensitive switching device fabricated with a metal complex with H ₂ L ^{SAL} . | Scheme S1. |
| 5. Cu(II)-complexes and Schiff base ligands bandgap value ensure semiconductor. | Table S1. |
| 6. Selected some important bond distances (Å) and angles (°) in the complex. | Table S2 |
| 7. Schiff base metal complexes utilized in the making of electrical conductivity-based photosensitive switching devices. | Table S3 |
| 8. (a) The XPS spectral data of the Ligand and Cu(II)-complex (binding energy/BE (eV)). | Table S4 |
| (b) Different interaction energies of the molecular pairs in the complex (kJ/mol). | Table S5 |
| (c) Computed NBO parameters of the current compound. | Table S6 |
| (d) Charge conducting parameters of CTFD. | Table S7 |
| 9. (a) The absorbance spectrum (inset) and the optical Band gap of H ₂ L ^{SAL} and the complex from Tauc's plots. | FIGURE S1A. |
| (b) IR spectrum of H ₂ L ^{SAL} . | FIGURE S1B. |

- (c) Capacitance vs. Frequency graph of **CTFD**. **FIGURE S1C.**
10. IR spectrum of complex. **FIGURE S2.**
11. Raman spectrum of the complex. **FIGURE S3.**
12. Ligand ($\text{H}_2\text{L}^{\text{SAL}}$) UV-Visible spectrum. **FIGURE S4.**
- 13.. Complex UV-Visible spectrum. **FIGURE S5.**
14. Complex DRS spectrum. **FIGURE S6.**
15. ^1H NMR spectra of $\text{H}_2\text{L}^{\text{SAL}}$. **FIGURE S7.**
16. ^{13}C NMR spectra of $\text{H}_2\text{L}^{\text{SAL}}$. **FIGURE S8.**
17. ^1H NMR spectra of complex. **FIGURE S9.**
18. Complex EDX profiles. **FIGURE S10.**
19. SEM micrographs (1-6) for $\text{H}_2\text{L}^{\text{SAL}}$. **FIGURE S11.**
20. SEM micrographs (1-6) for the copper complex. **FIGURE S12.**
21. Copper complex PXRD graph. **FIGURE S13.**
22. (a) XPS spectra of (1) O1s, (2) N1s, (3) C1s, and (4) Cu2p **FIGURE S14.**
22. ORTEP view of the complex. **FIGURE S15.**
23. QTAIM graph depicting BCPs of the studied complex. **FIGURE S16.**
24. $dV/dlnI$ vs. I and (B) H vs. I curve for **CTFD** under dark and **FIGURE S17A-17B.**
photo illumination conditions.
25. A probable mechanism of photosensitivity of the copper complex. **FIGURE S18.**

Section 1.1.

Optical Characterization

The optical band gap (E_g) was calculated using Tauc's equation (Equation S1).^{S1}

$$\alpha h\nu = A(h\nu - E_g)^n \quad (S1)$$

Where α , E_g , h , and ν stands for absorption coefficient, band gap, Planck's constant, and frequency of light. The exponent ' n ' is the electron transition processes dependent constant. ' A ' is a constant, considered as 1 for the ideal case. To calculate the direct optical bandgap the value of the exponent ' n ' in the above equation has been considered as $n = 1/2$.¹ By extrapolating the linear region of the plot $(\alpha h\nu)^2$ vs. $h\nu$ (Figure 1(A) and (B)) to absorptions, the values of optical direct band gap of the complex (E_{gC}) and the ligand (H_2L^{SAL}) (E_{gL}) have been calculated as 3.07 eV, and 3.09 eV (Figure 1(A) and (B) in the main manuscript).

Section 1.2.

Device Fabrication

In this study, multiple thin film devices were fabricated in ITO/synthesized Material (complex and ligand)/Al sandwich structure to perform the electrical research. In this regard, well dispersion of the synthesized complex and ligand was made in N, N-dimethyl formamide (DMF) by mixing and sonicating the Complex's equal and right proportion (15 mg/ml) in a vial. This prepared stable dispersion of the compound was deposited on the top of the ITO-coated glass substrate by spinning at 700 rpm for 5 minutes and, after that, at 1000 rpm for another 5 minutes with the help of the SCU 2700 spin coating unit. Afterwards, the as-deposited thin film was dried in a vacuum oven at 75 °C for several minutes to evaporate the solvent part fully. Here, we used aluminium as the metal electrode and deposited it on a dried thin film of prepared complexes in the thermal vapour deposition Unit. Here, **CTFD** represents the thin

film device made from Complex, and **LTFD** is the thin film device made from ligand, respectively. The source meter (made by Keithley Model No: 2400) and two probe techniques have been implemented to collect the fabricated devices' current-voltage (I - V) features, helping to determine the electrical properties. In the experiment section, the light source used for electrical characterization is a 300 W ozone-free Xenon arc lamp, which emits broadband white light ranging from 300-800 nm.

Section 1.3.

Optical Characterization

The I - V characteristic of **CTFD** was further analyzed by thermionic emission theory. Cheung's method has also been employed to extract important diode parameters.^{S1} In this regard, the obtained I - V curve was analyzed quantitatively by considering the following standard equations:^{S1, S2}

$$I = I_0 \exp\left(\frac{qV}{\eta kT}\right) \left[1 - \exp\left(\frac{-qV}{\eta kT}\right)\right] \quad (S2)$$

$$I_0 = AA^* T^2 \exp\left(\frac{-q\phi_B}{kT}\right) \quad (S3)$$

where, I_0 , k , T , V , A , η , and A^* stands for saturation current, electronic charge, the Boltzmann constant, temperature in Kelvin, forward bias voltage, effective diode area, ideality factor, and effective Richardson constant, respectively. The effective diode area has been estimated as $7.065 \times 10^{-2} \text{ cm}^2$ and the effective Richardson constant has been considered as $32 \text{ AK}^{-2} \text{ cm}^{-2}$ for all the devices. The series resistance, ideality factor, and barrier potential height were also determined by using equations S4 to S6, which were extracted from Cheung's idea,^{S3, S4}

$$\frac{dV}{d \ln(I)} = \left(\frac{\eta kT}{q}\right) + IR_s \quad (S4)$$

$$H(I) = V - \left(\frac{\eta kT}{q} \right) \ln \left(\frac{I_S}{AA^* T^2} \right)$$

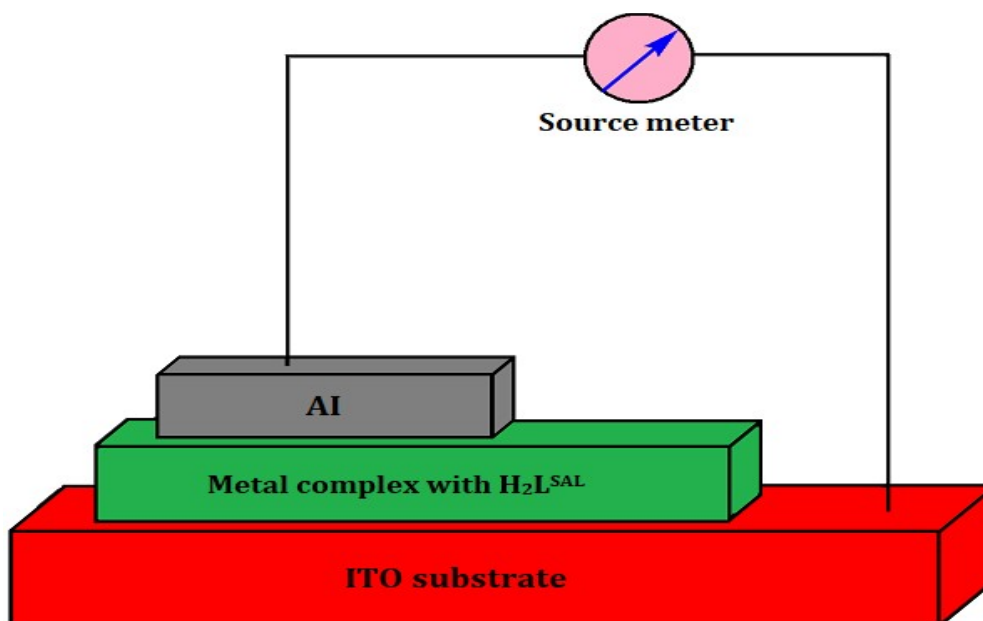
(S5)

$$H(I) = IR_S + \eta\phi_B \quad (S6)$$

From the saturated values of capacitance at the higher frequency regime, (Figure S1) the dielectric permittivity of the complex was calculated using the following equation:^{S1}

$$\epsilon_r = \frac{1}{\epsilon_0} \frac{C \cdot D}{A} \quad (S7)$$

where, C is the capacitance (at saturation), D is the thickness of the film which has been considered as $\sim 1 \mu\text{m}$ and A is the effective area. Using the above formula, the relative dielectric constant of the Complex has been estimated as 5.35×10^{-1} .



Scheme S1. Schematic depiction of an electrical conductivity-based photo-sensitive switching device fabricated with a Metal-complex with $\text{H}_2\text{L}^{\text{SAL}}$.

Table S1 Published Cu(II)-complexes and Schiff base ligands (L) bandgap value ensure semiconductor function.

Complexes	Optical band gap value (eV)	References
[Cu(L) μ -1,1-N ₃]	2.84	1
[Cu(fum)(4-phpy) ₂ (H ₂ O)]	2.67	2
[Cu(nip)(4-brpy) ₂]	3.97	3
[Cu ₂ (adc)(4-pic) ₆ (H ₂ O) ₄][ClO ₄] ₂	3.10	4
[Cu ₂ (bpd) ₂ (nac) ₂].2CH ₃ CN.2H ₂ O	3.46	5
[CuL(NCS)]	2.99	6
[Cu ₂ L ₂ (μ -1,3-SCN) ₂] _n	2.95	7
[CuL ¹ (μ -1,3-N ₃)] _∞	2.91	8
[Cu ₂ L ² (μ -1,1-N ₃)(μ -1,3-N ₃)] _∞	2.89	
Schiff base [1,4-bis-(quinolin-6-yliminomethyl) benzene (BQB)]	3.46	9
Schiff base [<i>N</i> - <i>N</i> -(1,2-diphenyl ethane-1,2-diylidene)bis(3-Nitrobenzohydrazide)]	2.67	10
H₂L^{SAL}	3.09	This work
[Cu₂(L^{SAL})₂]	3.07	This work

Table S2 Selected some important bond distances (Å) and angles (°) in the complex.

Atom	Atom	Length/Å	Atom	Atom	Length/Å
Cu1	N1	1.953 (2)	C6	C5	1.417 (4)
Cu1	O1	1.9073 (18)	C1	C2	1.408 (4)
Cu1	O2 ¹	2.4120 (17)	C2	C3	1.375 (4)
Cu1	O2	1.9406 (17)	C3	C4	1.388 (5)
Cu1	N2	1.948 (2)	C4	C5	1.360 (5)
N1	C7	1.287 (3)	C8	C9	1.516 (4)
N1	C8	1.470 (3)	C10	C11	1.430 (4)
O1	C1	1.310 (3)	C11	C16	1.417 (4)
O2	C16	1.324 (3)	C11	C12	1.411 (4)
N2	C9	1.455 (3)	C16	C15	1.404 (4)
N2	C10	1.289 (3)	C15	C14	1.388 (4)
C7	C6	1.425 (4)	C14	C13	1.382 (5)
C6	C1	1.425 (4)	C13	C12	1.357 (5)

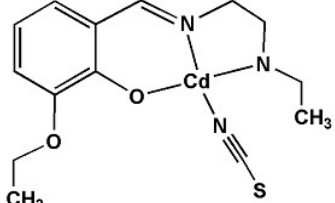
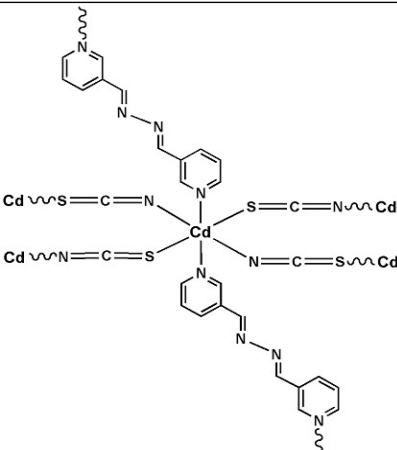
$$1=3/2-x,1/2-y,1-z$$

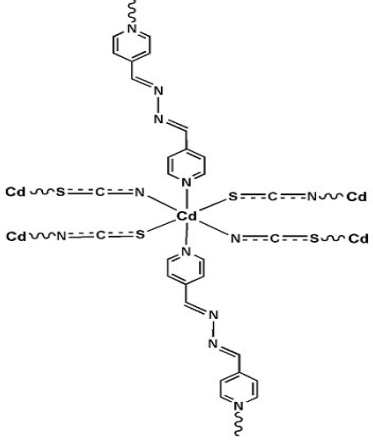
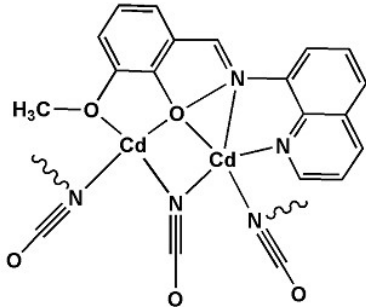
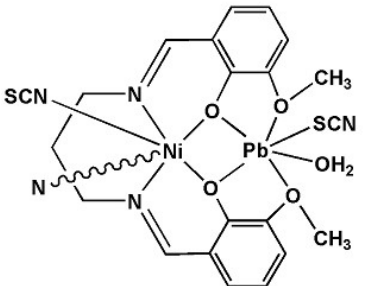
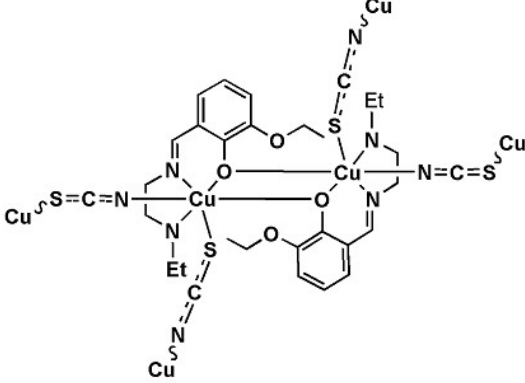
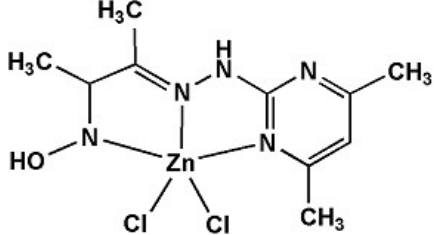
Atom	Atom	Atom	Angle/°	Atom	Atom	Atom	Angle/°
N1	Cu1	O2 ¹	102.38 (7)	C5	C6	C7	117.6 (3)
O1	Cu1	N1	92.77 (8)	C5	C6	C1	119.1 (3)
O1	Cu1	O2 ¹	93.90 (7)	O1	C1	C6	124.5 (2)
O1	Cu1	O2	91.13 (7)	O1	C1	C2	118.5 (2)
O1	Cu1	N2	171.09 (8)	C2	C1	C6	116.9 (2)
O2	Cu1	N1	170.32 (8)	C3	C2	C1	122.1 (3)
O2	Cu1	O2 ¹	86.17 (7)	C2	C3	C4	120.8 (3)
O2	Cu1	N2	91.44 (8)	C5	C4	C3	119.0 (3)
N2	Cu1	N1	83.42 (9)	C4	C5	C6	122.1 (3)
N2	Cu1	O2 ¹	94.78 (8)	N1	C8	C9	108.0 (2)
C7	N1	Cu1	126.68 (19)	N2	C9	C8	107.3 (2)
C7	N1	C8	119.6 (2)	N2	C10	C11	124.6 (2)
C8	N1	Cu1	113.59 (17)	C16	C11	C10	123.3 (2)
C1	O1	Cu1	126.93 (17)	C12	C11	C10	117.8 (3)
Cu1	O2	Cu1 ¹	93.83 (7)	C12	C11	C16	118.9 (3)

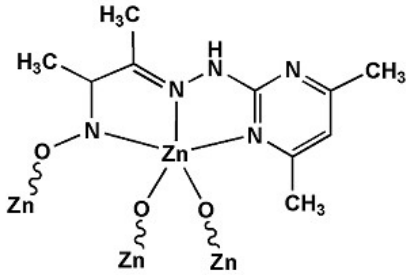
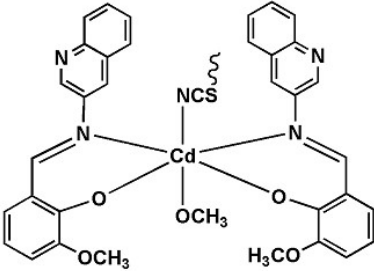
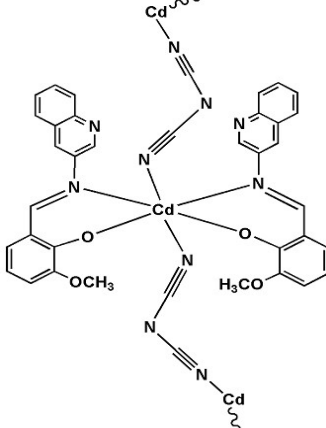
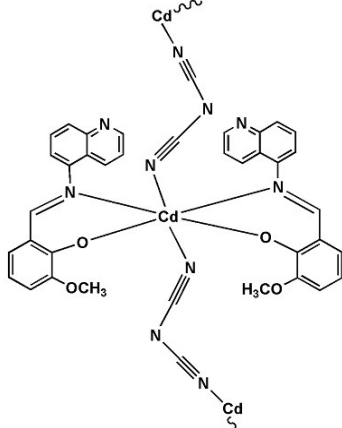
Atom	Atom	Atom	Angle/°	Atom	Atom	Atom	Angle/°
C16	O2	Cu1	125.17 (16)	O2	C16	C11	124.2 (2)
C16	O2	Cu1 ¹	110.16 (14)	O2	C16	C15	117.8 (2)
C9	N2	Cu1	111.96 (17)	C15	C16	C11	118.0 (2)
C10	N2	Cu1	126.41 (19)	C14	C15	C16	121.1 (3)
C10	N2	C9	121.2 (2)	C13	C14	C15	120.6 (3)
N1	C7	C6	124.8 (2)	C12	C13	C14	119.5 (3)
C1	C6	C7	123.2 (2)	C13	C12	C11	122.0 (3)

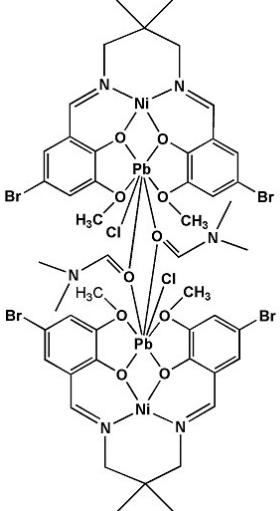
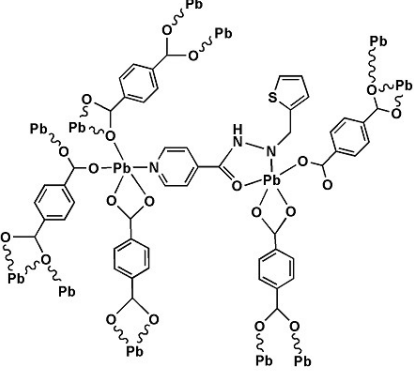
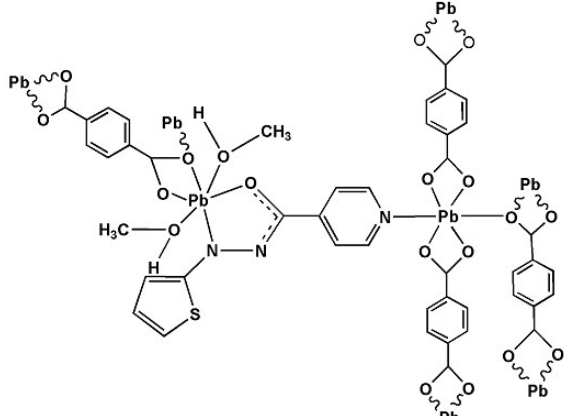
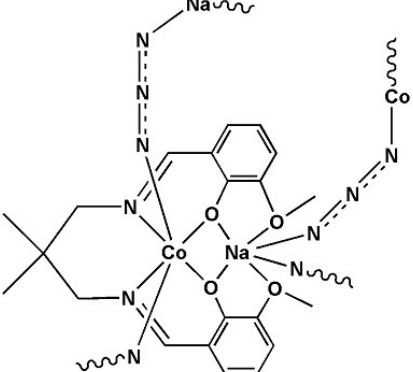
$$1=3/2-x, 1/2-y, 1-z$$

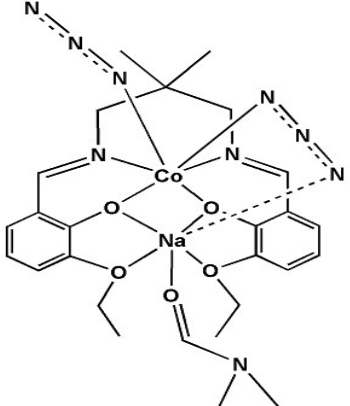
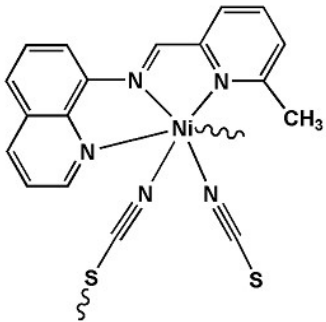
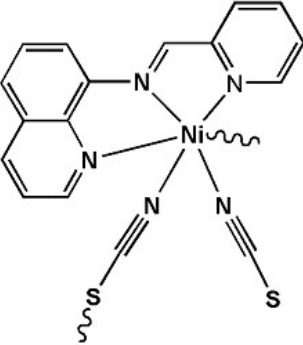
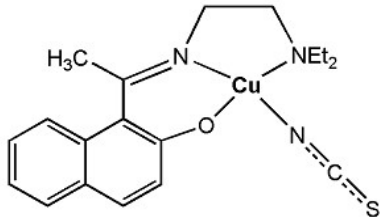
Table S3 Schiff base metal complexes utilized in the making of electrical conductivity-based photosensitive switching devices.

SL No.	Structure	Conductivity (under dark) (S m ⁻¹)	Conductivity (in light) (S m ⁻¹)	Ref
1		1.01×10^{-6}	2.16×10^{-6}	11
2		4.53×10^{-5}	1.93×10^{-4}	12

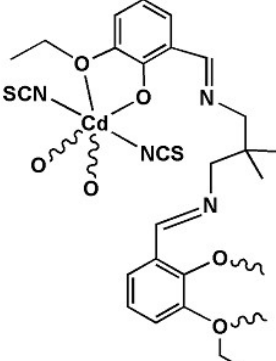
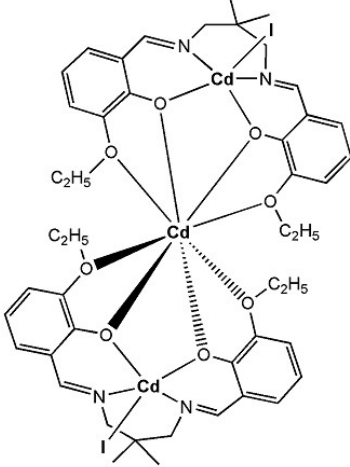
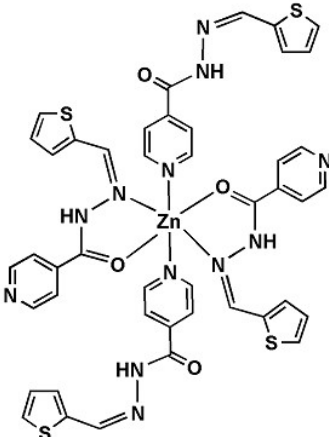
3		2.90×10^{-4}	7.16×10^{-4}	13
4		8.26×10^{-2}	22.07×10^{-2}	14
5		2.02×10^{-2}	8.55×10^{-2}	15
6		3.63×10^{-3}	4.13×10^{-3}	16
7		2.13×10^{-3}	3.19×10^{-3}	17

8		3.99×10^{-3}	7.13×10^{-3}	18
9		1.26×10^{-6}	6.72×10^{-5}	19
10		1.07×10^{-7}	2.44×10^{-7}	20
11		1.78×10^{-7}	6.15×10^{-7}	21

12		7.47×10^{-4}	23.12×10^{-4}	22
13		2.94×10^{-6}	6.12×10^{-6}	23
14		2.92×10^{-7}	3.66×10^{-7}	24
15		0.88×10^{-8}	2.38×10^{-8}	25

16		8.24×10^{-5}	14.03×10^{-5}	26
17		7.0×10^{-5}	3.5×10^{-4}	27
18		2.0×10^{-5}	4.9×10^{-4}	28
19		6.49×10^{-4}	21.29×10^{-4}	29

20		13.1×10^{-6}	11.2×10^{-5}	30
21		5.4×10^{-6}	13.5×10^{-5}	31
22		0.87×10^{-3}	2.45×10^{-3}	32

23		3.89×10^{-4}	8.25×10^{-4}	33
24		1.81×10^{-4}	4.72×10^{-4}	34
25		8.07×10^{-3}	9.26×10^{-3}	35

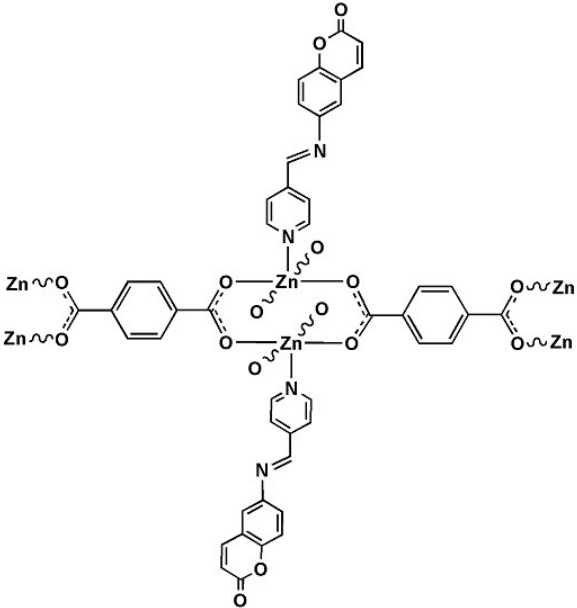
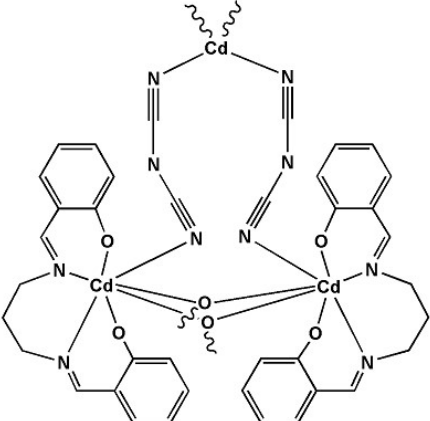
26		2.53×10^{-9}	5.97×10^{-5}	36
27		3.69×10^{-4}	10.68×10^{-4}	37
28	[Cu₂(L^{SAL})]	2.41×10^{-7}	4.27×10^{-7}	This work

Table S4 The XPS spectral data of the Ligand and Cu(II)-complex (binding energy/BE (eV))

Compounds	C1s	O1s	N1s	Cl1s	Cu2p
L (Common Salen ligand)	285.1	530.3	398.8	--	-
	286.0	532.2 533.8	402.2		
Cu-complex	285.74	532.16	399.64	--	935.31
			402.01		954.80

Table S5 Different interaction energies of the molecular pairs in the complex (kJ/mol).

N	Symmetry Operations	R(Å)	Electron Density	E_{ele}	E_{pol}	E_{dis}	E_{rep}	E_{tot}
2	x,y,z	6.98	HF/3-21G	-25.6	-10.9	-35.0	16.5	-51.4
1	-x+1/2, -y+1/2, -z	7.97	HF/3-21G	8.3	-2.1	-18.5	11.1	-0.6
1	-x,-y,-z	13.05	HF/3-21G	-4.5	-0.8	-9.4	3.6	-10.7
2	x+1/2, y+1/2, z	13.76	HF/3-21G	1.7	-0.4	-7.6	3.3	-2.7
2	-x+1/2, y+1/2, -z+1/2	5.19	HF/3-21G	-8.3	-13.6	-66.4	34.1	-49.5
1	-x+1/2, -y+1/2, -z	3.68	HF/3-21G	-108.8	-59.6	-100.3	117.1	-145.0
2	x+1/2, y+1/2, z	13.76	HF/3-21G	0.4	-0.5	-9.0	4.9	-4.1
1	-x, y, -z+1/2	13.57	HF/3-21G	1.1	-0.4	-4.5	0.5	-2.8
1	-x+1/2, -y+1/2, -z	7.80	HF/3-21G	-5.1	-2.5	-10.8	2.9	-14.2
1	-x, y, -z+1/2	14.14	HF/3-21G	0.2	-0.2	-4.6	1.6	-2.8

Table S6 Computed NBO parameters of the copper complex.

Donor (i)	Type of Bond	Occupancy	Acceptor (j)	Type of Bond	Occupancy	E⁽²⁾ (Kcal/mol)	ε(j)-ε(i) (a.u)	F(i, j) (a.u)
Cu 1	LP*(6)	0.26628	Cu 1	LP*(8)	0.12054	11.41	0.04	0.043
	LP*(6)	0.26628	Cu 1	RY*(1)	0.00128	19.54	2.75	0.565
	LP*(6)	0.26628	Cu 1	RY*(3)	0.00067	14.09	1.33	0.334
	LP*(6)	0.26628	Cu 1	RY*(7)	0.12335	17.82	0.23	0.156
	LP*(6)	0.26628	Cu 1	RY*(8)	0.12054	15.36	2.74	0.501
N 2	LP (1)	1.72921	Cu 1	LP*(5)	1.56245	18.78	0.13	0.074
	LP (1)	1.72921	Cu 1	LP*(6)	0.26628	40.50	0.63	0.143
	LP (1)	1.72921	Cu 1	LP*(8)	0.12054	17.46	0.67	0.100
O 3	LP (1)	1.92365	Cu 1	LP*(7)	0.12335	15.45	0.78	0.099
	LP (1)	1.92365	Cu 1	LP*(8)	0.12054	11.94	0.81	0.089
	LP (2)	1.76286	Cu 1	LP*(5)	1.56245	15.12	0.12	0.067
	LP (2)	1.76286	Cu 1	LP*(6)	0.26628	27.18	0.63	0.117
	LP (2)	1.76286	Cu 1	LP*(7)	0.12335	19.85	0.63	0.103
O 4	LP (1)	1.92236	Cu 1	LP*(8)	0.12054	24.07	0.81	0.126
	LP (2)	1.76758	Cu 1	LP*(5)	1.56245	14.78	0.13	0.067
	LP (2)	1.76758	Cu 1	LP*(6)	0.26628	28.38	0.63	0.121
	LP (2)	1.76758	Cu 1	LP*(8)	0.12054	17.50	0.64	0.100
N 5	LP (1)	1.71887	Cu 1	LP*(5)	1.56245	19.43	0.13	0.074
	LP (1)	1.71887	Cu 1	LP*(6)	0.26628	40.11	0.63	0.142
	LP (1)	1.71887	Cu 1	LP*(7)	0.12335	18.00	0.63	0.099

C8 - C9	π	1.54028	N 2 - C 6	π	1.94646	33.50	0.22	0.081
	π	1.54028	C 10 - C 12	π	1.73271	13.48	0.28	0.057
	π	1.54028	C 14 - C 16	π	1.72695	24.18	0.28	0.076
C10 - C12	π	1.73271	C 8 - C 9	π^*	0.47296	21.68	0.28	0.073
	π	1.73271	C 14 - C 16	π^*	0.30060	15.58	0.29	0.060
C 14 - C16	π	1.72695	C 8 - C 9	π^*	0.47296	14.05	0.28	0.059
	π	1.72695	C 10 - C 12	π^*	0.28611	22.54	0.29	0.072
C 26 - C27	π	1.54207	N 5 - C 24	π^*	0.25302	32.56	0.23	0.081
	π	1.54207	C 28 - C 30	π^*	0.28968	13.61	0.28	0.057
	π	1.54207	C 32 - C 34	π^*	0.29859	24.10	0.28	0.076
C 28 - C30	π	1.73119	C 26 - C 27	π^*	0.46953	21.78	0.28	0.073
	π	1.73119	C 32 - C 34	π^*	0.29859	15.66	0.29	0.060
C32 - C 34	π	1.72195	C 26 - C 27	π^*	0.46953	14.22	0.28	0.059
	π	1.72195	C 28 - C 30	π^*	0.28968	22.82	0.28	0.072
O 3	LP (3)	1.70074	C 8 - C 9	π^*	0.47296	52.15	0.28	0.113
O 4	LP (3)	1.70255	C 26 - C 27	π^*	0.46953	50.79	0.29	0.112
N 2 - C 6	π^*	0.26037	C 8 - C 9	π^*	0.47296	65.66	0.04	0.078
N 5 - C24	π^*	0.25302	C 26 - C 27	π^*	0.46953	66.61	0.04	0.077
C 8 - C 9	π^*	0.47296	C 10 - C 12	π^*	0.28611	287.72	0.01	0.080
	π^*	0.47296	C 14 - C 16	π^*	0.30060	260.58	0.01	0.076
C 26 - C27	π^*	0.46953	C 32 - C 34	π^*	0.29859	262.99	0.01	0.076
Cu 36	LP*(6)	0.26625	Cu 36	LP*(8)	0.12054	11.41	0.04	0.043
	LP*(6)	0.26625	Cu 36	RY*(1)	0.00128	19.52	2.75	0.565
	LP*(6)	0.26625	Cu 36	RY*(3)	0.00067	14.07	1.32	0.333
	LP*(6)	0.26625	Cu 36	RY*(7)	0.00027	17.73	0.23	0.155
	LP*(6)	0.26625	Cu 36	RY*(8)	0.00019	15.36	2.74	0.502
N 37	LP (1)	1.72927	Cu 36	LP*(6)	0.26625	40.50	0.63	0.143
	LP (1)	1.72927	Cu 36	LP*(8)	0.12054	17.45	0.67	0.100
O 38	LP (1)	1.92366	Cu 36	LP*(7)	0.12332	15.42	0.78	0.099
	LP (1)	1.92366	Cu 36	LP*(8)	0.12054	11.95	0.81	0.089
	LP (2)	1.76288	Cu 36	LP*(6)	0.26625	27.22	0.63	0.118
	LP (2)	1.76288	Cu 36	LP*(7)	0.12332	19.83	0.63	0.103
O 39	LP (1)	1.92236	Cu 36	LP*(8)	0.12054	24.05	0.81	0.126
	LP (2)	1.70255	Cu 36	LP*(6)	0.26625	28.37	0.63	0.121
	LP (2)	1.76765	Cu 36	LP*(8)	0.12054	17.49	0.67	0.099
N 40	LP (1)	1.71894	Cu 36	LP*(6)	0.26625	40.10	0.63	0.142
	LP (1)	1.71894	Cu 36	LP*(7)	0.12332	17.99	0.63	0.099
C 45 - C47	π	1.73270	C 43 - C 44	π^*	0.47295	21.68	0.28	0.073
	π	1.73270	C 49 - C 51	π^*	0.30059	15.58	0.29	0.060
C49 - C 51	π	1.72695	C 43 - C 44	π^*	0.47295	14.05	0.28	0.059
	π	1.72695	C 45 - C 47	π^*	0.28613	22.54	0.29	0.072
C 61 - C 62	π	1.54208	N 40 - C 59	π^*	0.01792	32.55	0.23	0.081
	π	1.54208	C 63 - C 65	π^*	0.28966	13.61	0.28	0.057
	π	1.54208	C 67 - C 69	π^*	0.29863	24.10	0.28	0.076
C 63 - C65	π	1.97929	C 61 - C 62	π^*	0.05068	21.78	0.28	0.073
	π	1.97929	C 67 - C 69	π^*	0.29863	15.66	0.29	0.060
C67 - C 69	π	1.72198	C 61 - C 62	π^*	0.05068	14.22	0.28	0.059

	π	1.72198	C 63 - C 65	π^*	0.28966	22.82	0.28	0.072
O 38	LP (3)	1.70080	C 43 - C 44	π^*	0.47295	52.20	0.28	0.113
O 39	LP (3)	1.70255	C 61 - C 62	π^*	0.46954	50.81	0.29	0.112
N37 - C41	π^*	0.26041	C 43 - C 44	π^*	0.47295	65.67	0.04	0.078
N40 - C59	π^*	0.01792	C 61 - C 62	π^*	0.46954	66.60	0.04	0.077
C43 - C 44	π^*	0.47295	C 45 - C 47	π^*	0.28613	287.75	0.01	0.080
	π^*	0.47295	C 49 - C 51	π^*	0.30059	260.56	0.01	0.076
	π	1.54027	N 37 - C 41	π^*	0.26041	33.51	0.22	0.081
	π	1.54027	C 45 - C 47	π^*	0.28613	13.48	0.28	0.057
	π	1.54027	C 49 - C 51	π^*	0.30059	24.18	0.28	0.076
C61 - C 62	π^*	0.46954	C 67 - C 69	π^*	0.29863	263.12	0.01	0.076

Table S7 Charge conducting parameters of CTFD.

Condition	ϵ_r	μ_{eff} ($m^2V^{-1}s^{-1}$)	τ (sec)	D	L_D (m)
Dark		8.25×10^{-6}	3.44×10^{-8}	1.62×10^{-5}	1.207×10^{-7}
Light	5.35×10^{-1}	2.11×10^{-5}	1.35×10^{-8}	1.05×10^{-4}	1.212×10^{-7}

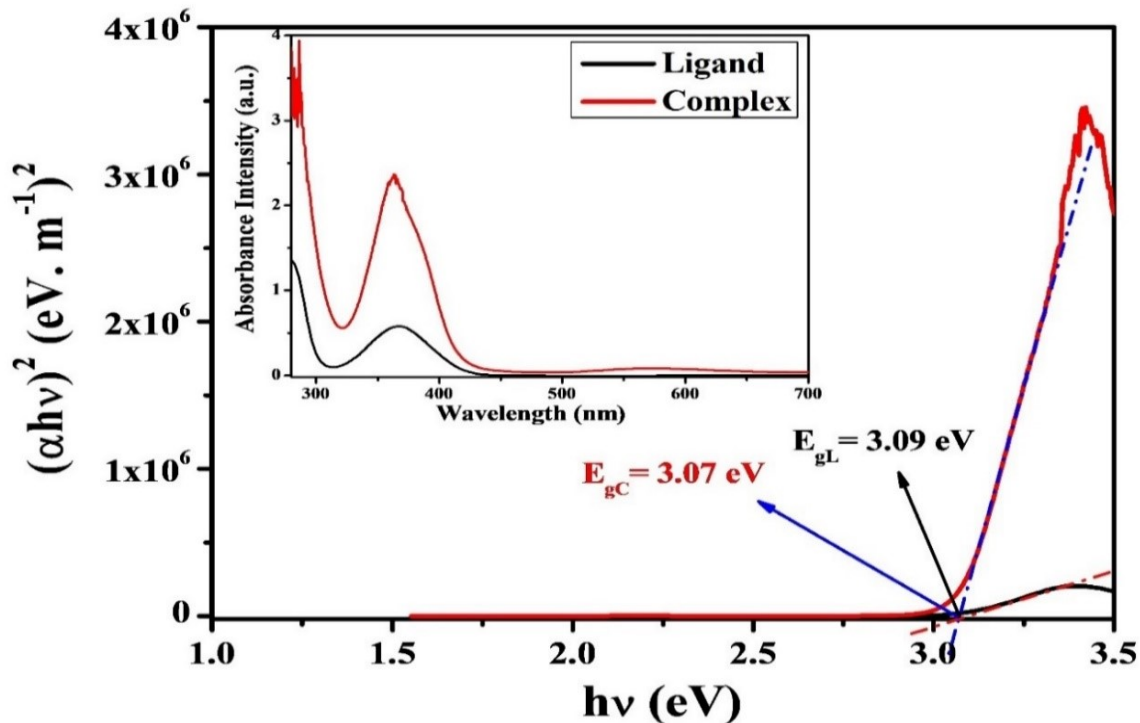


Fig.S1A. The absorbance spectrum (inset) and the optical Band gap of H_2L^{SAL} and the complex from Tauc's plots.

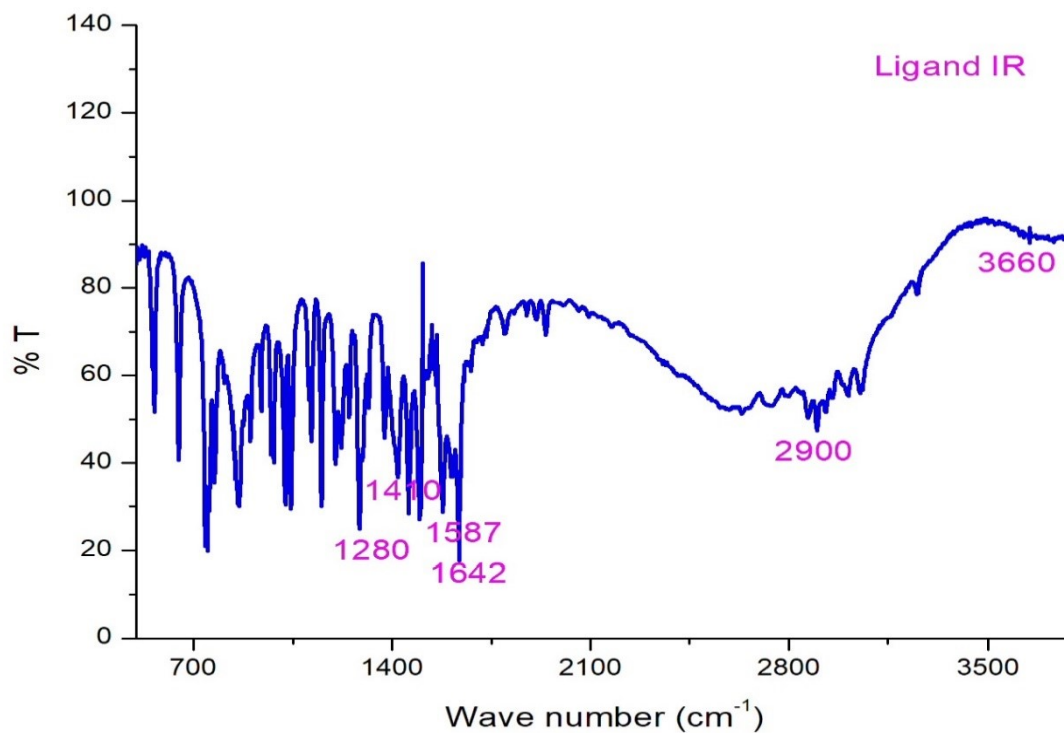


Fig.S1B. IR spectrum of H_2L^{SAL} .

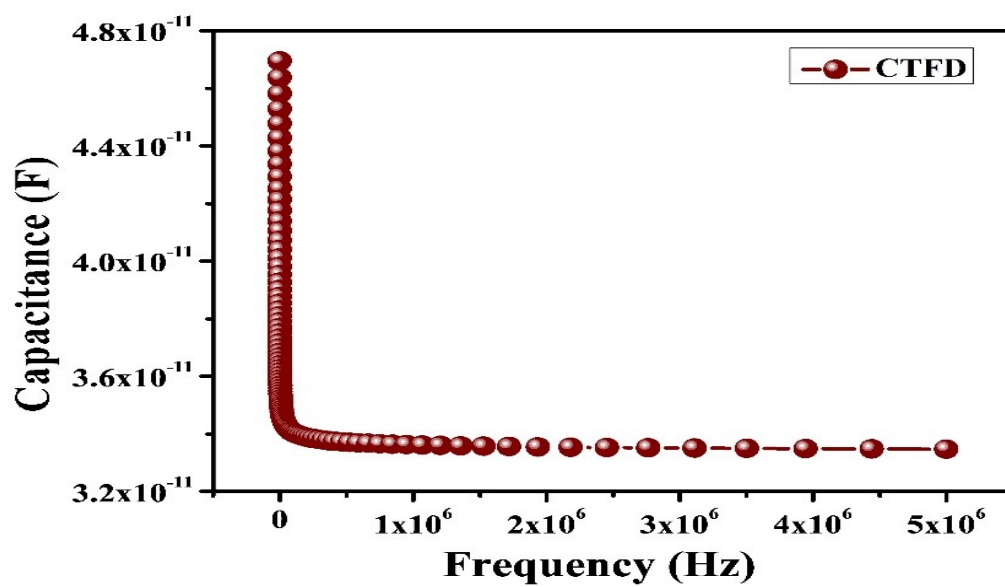


Fig.S1C. Capacitance vs. Frequency graph of CTFD.

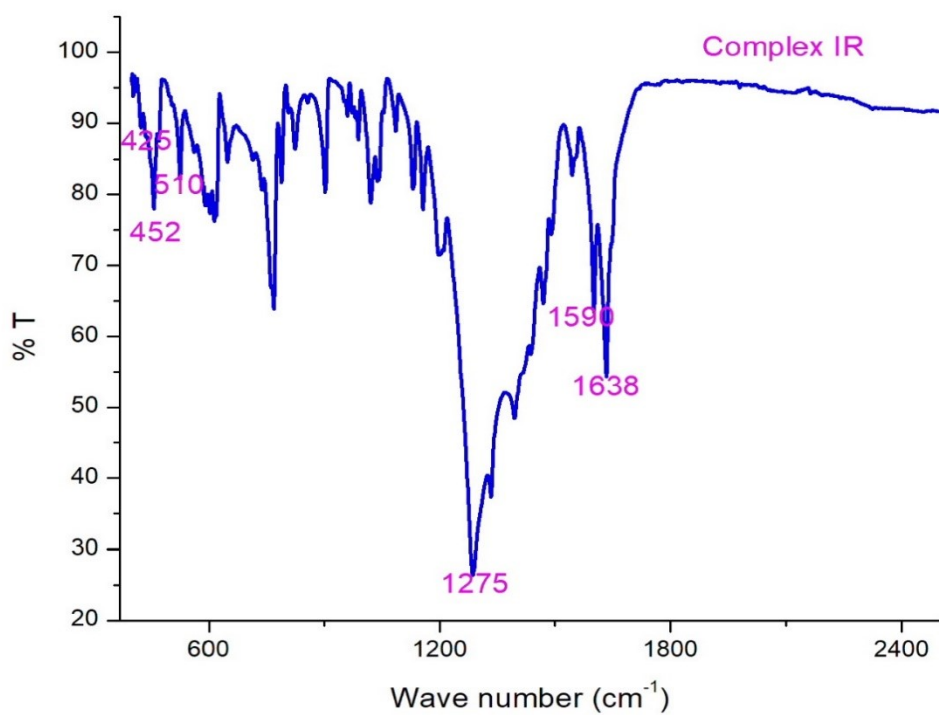
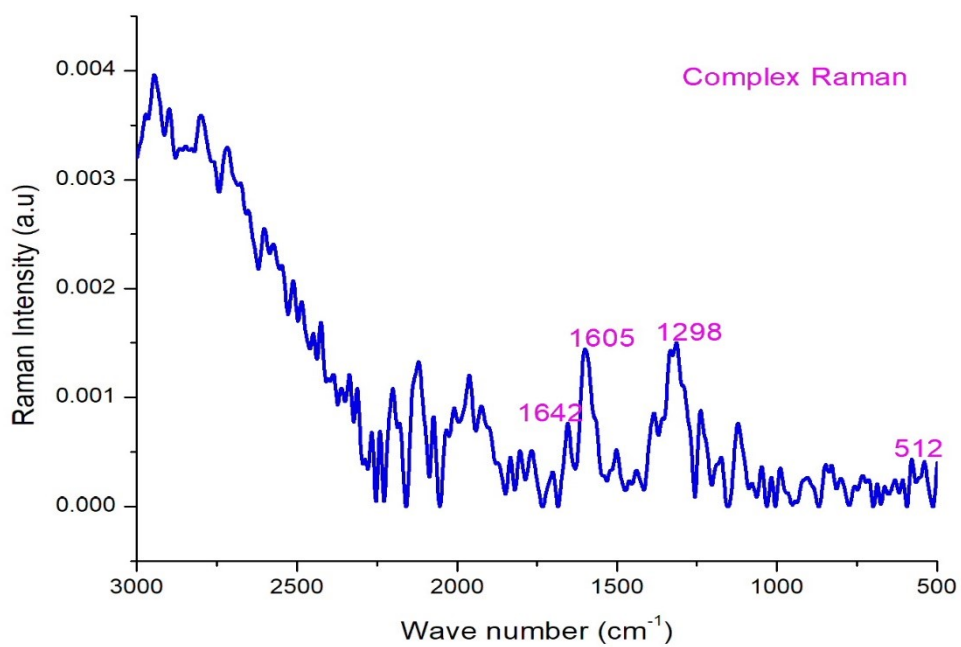


Fig.S2. IR spectrum of the complex.



g.S3. Raman spectrum of the complex.

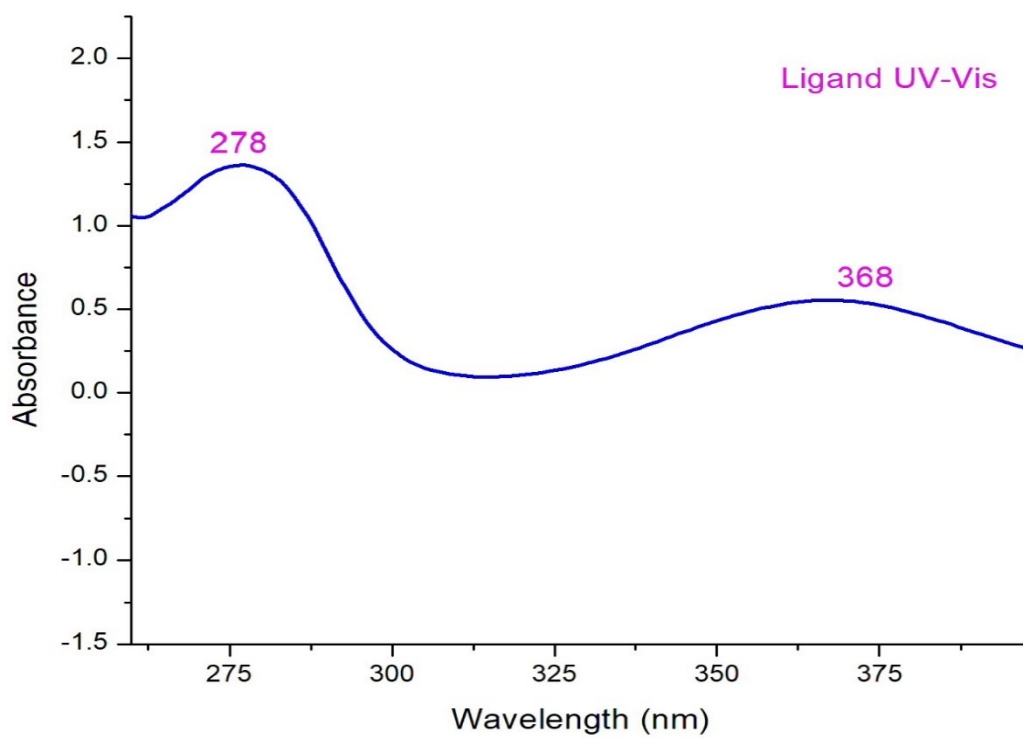


Fig.S4. Ligand (H_2L^{SAL}) UV-Visible spectrum.

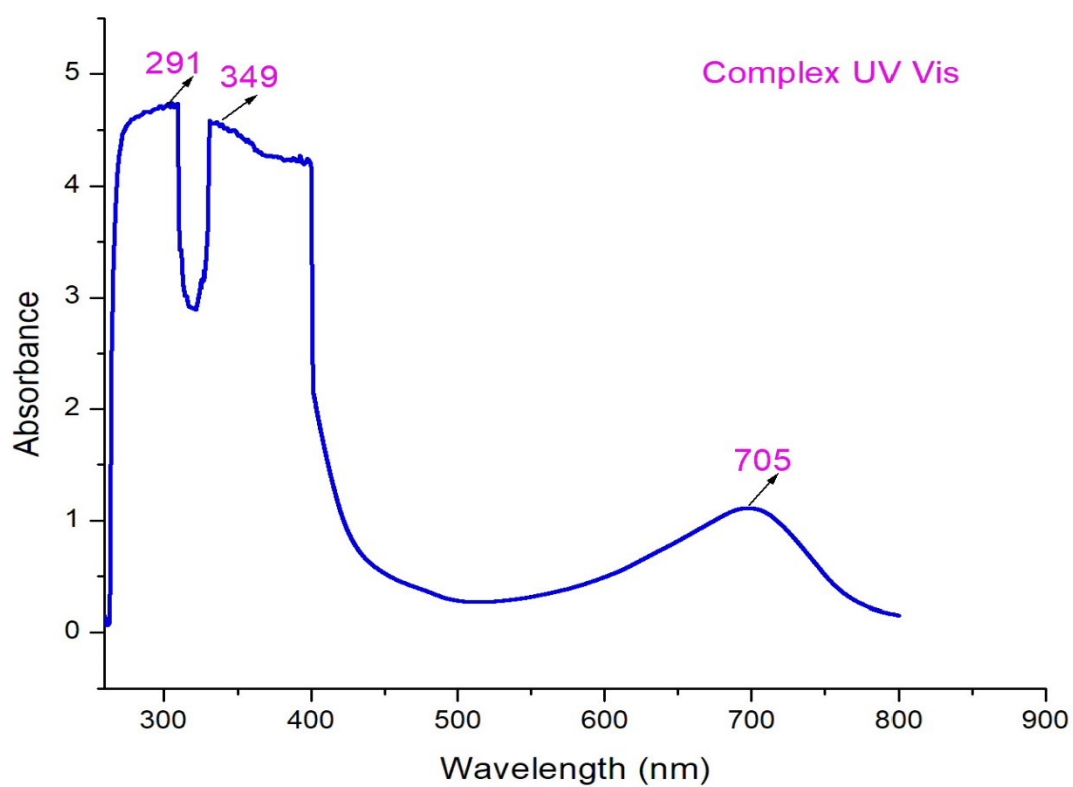


Fig.S5. Complex UV-Visible spectrum.

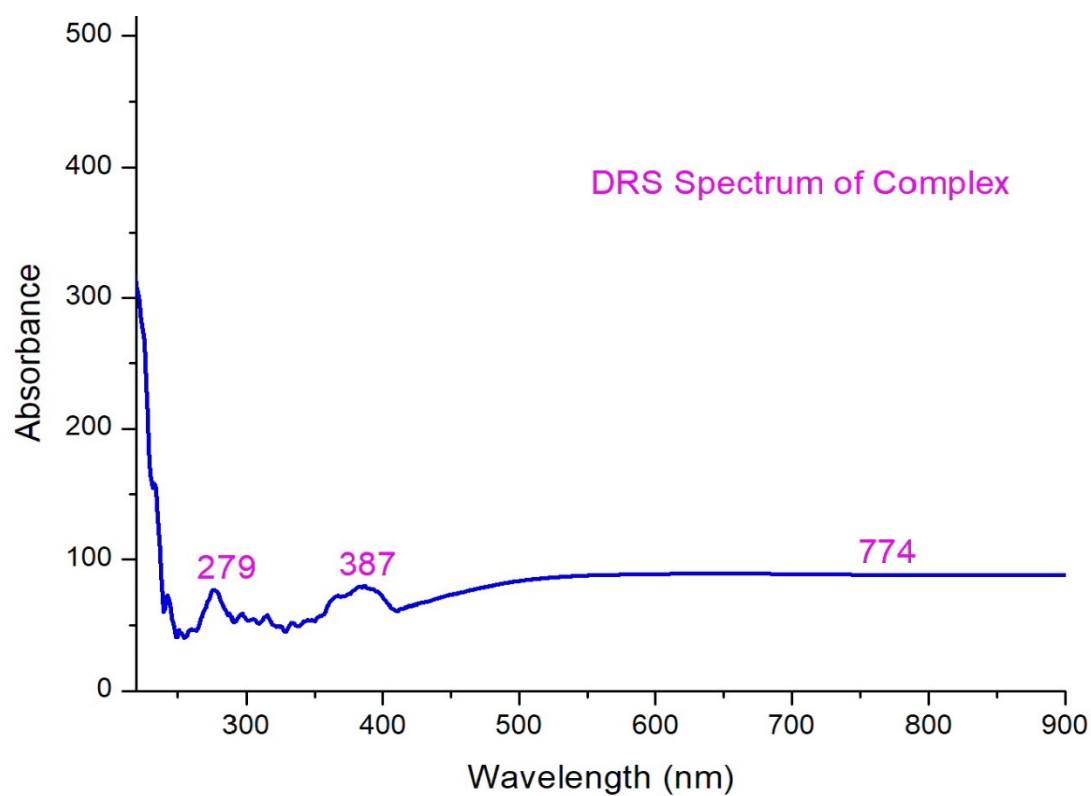


Fig.S6. Complex DRS spectrum.

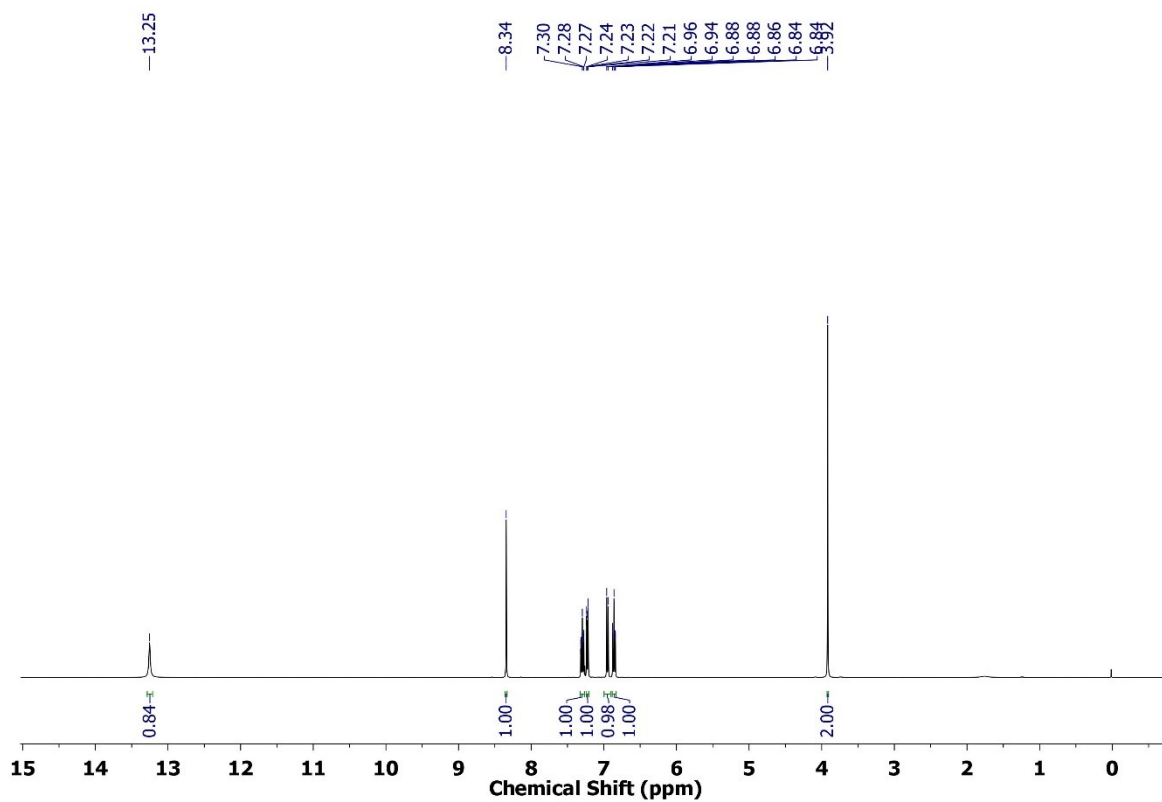


Fig.S7. ^1H NMR spectra of $\text{H}_2\text{L}^{\text{SAL}}$.

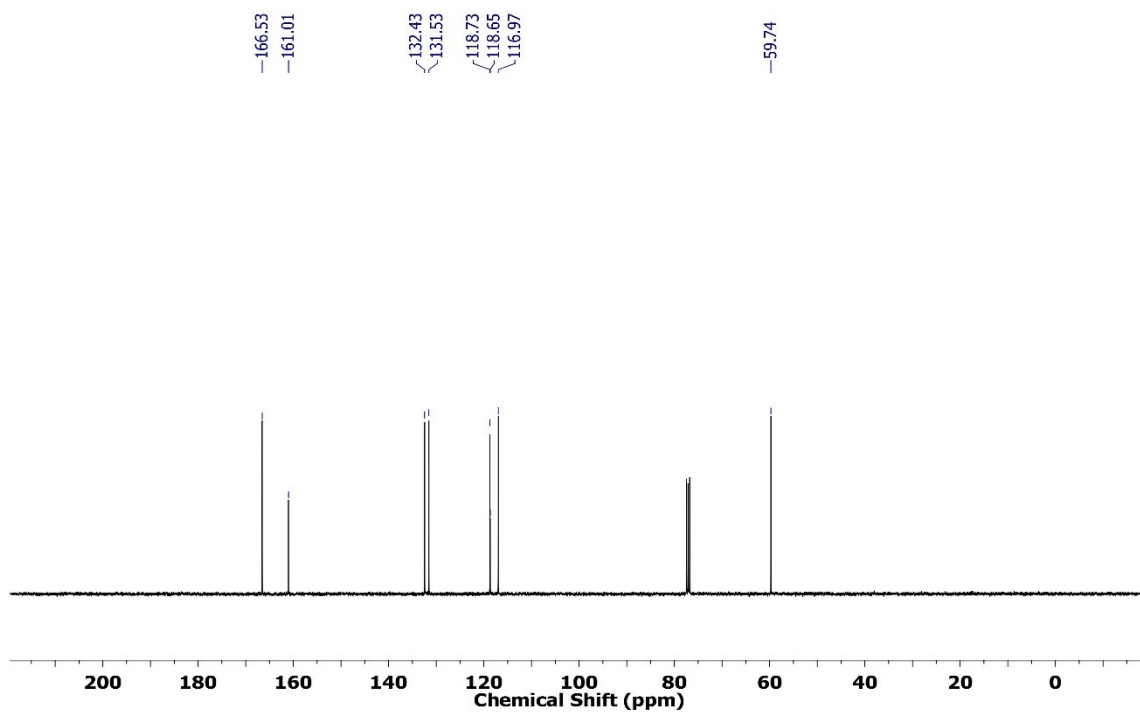


Fig.S8. ^{13}C NMR spectra of $\text{H}_2\text{L}^{\text{SAL}}$.

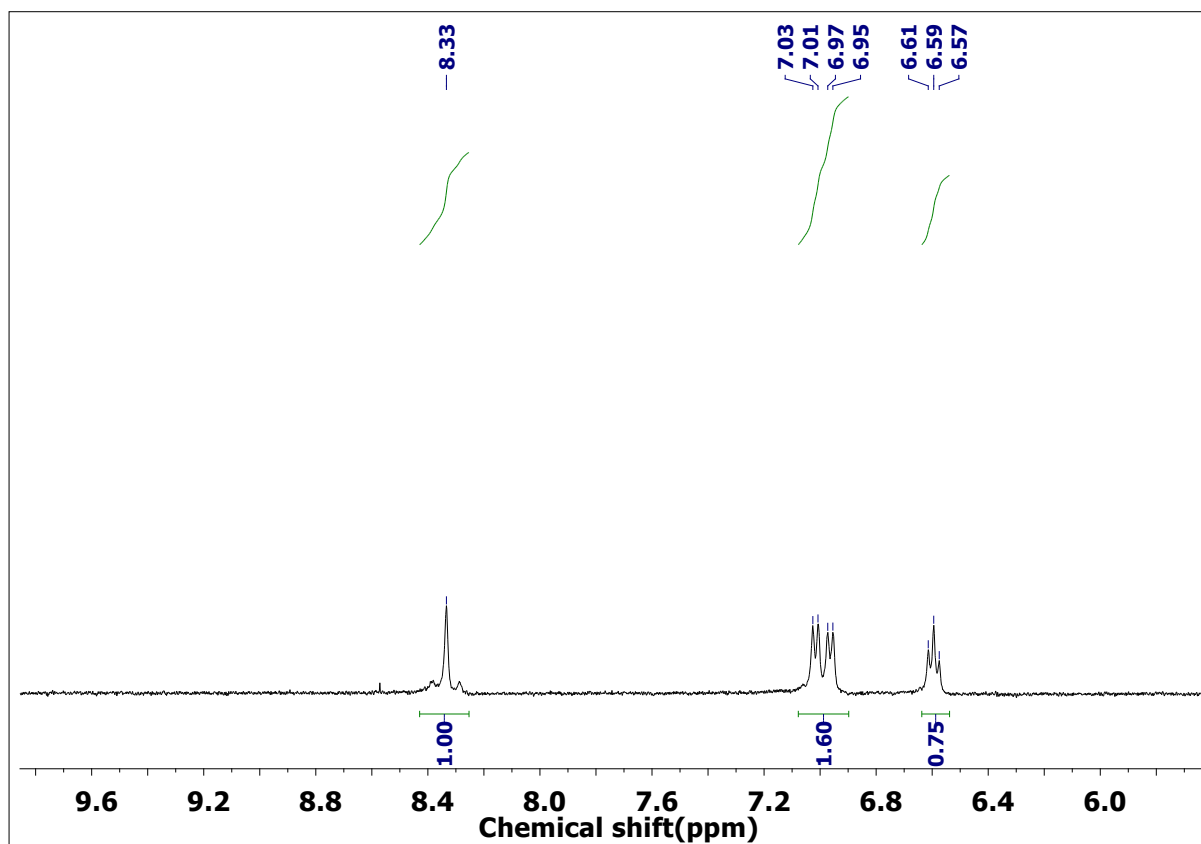


Fig.S9. ^1H NMR spectra of complex.

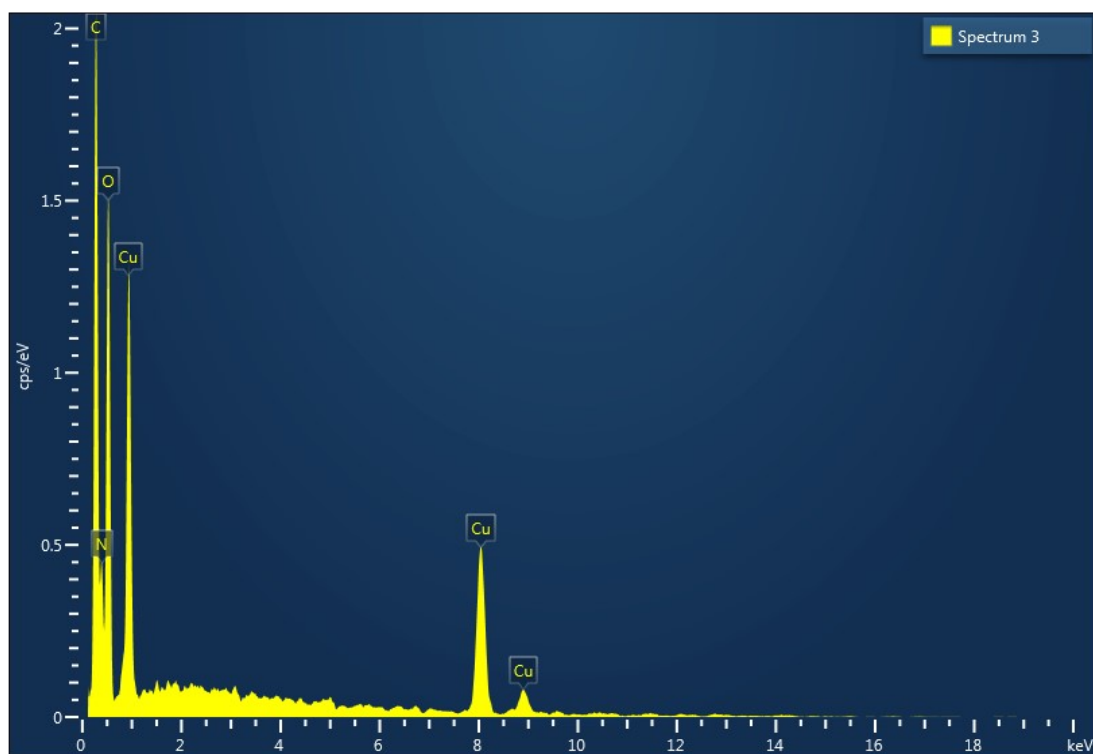


Fig.S10. Complex EDX profiles.

Element	Line Type	Wt. %	Atomic %
C	K series	38.59	51.31
N	K series	12.31	14.04
O	K series	29.87	29.82
Cu	K series	19.22	4.83
Total:		100	100

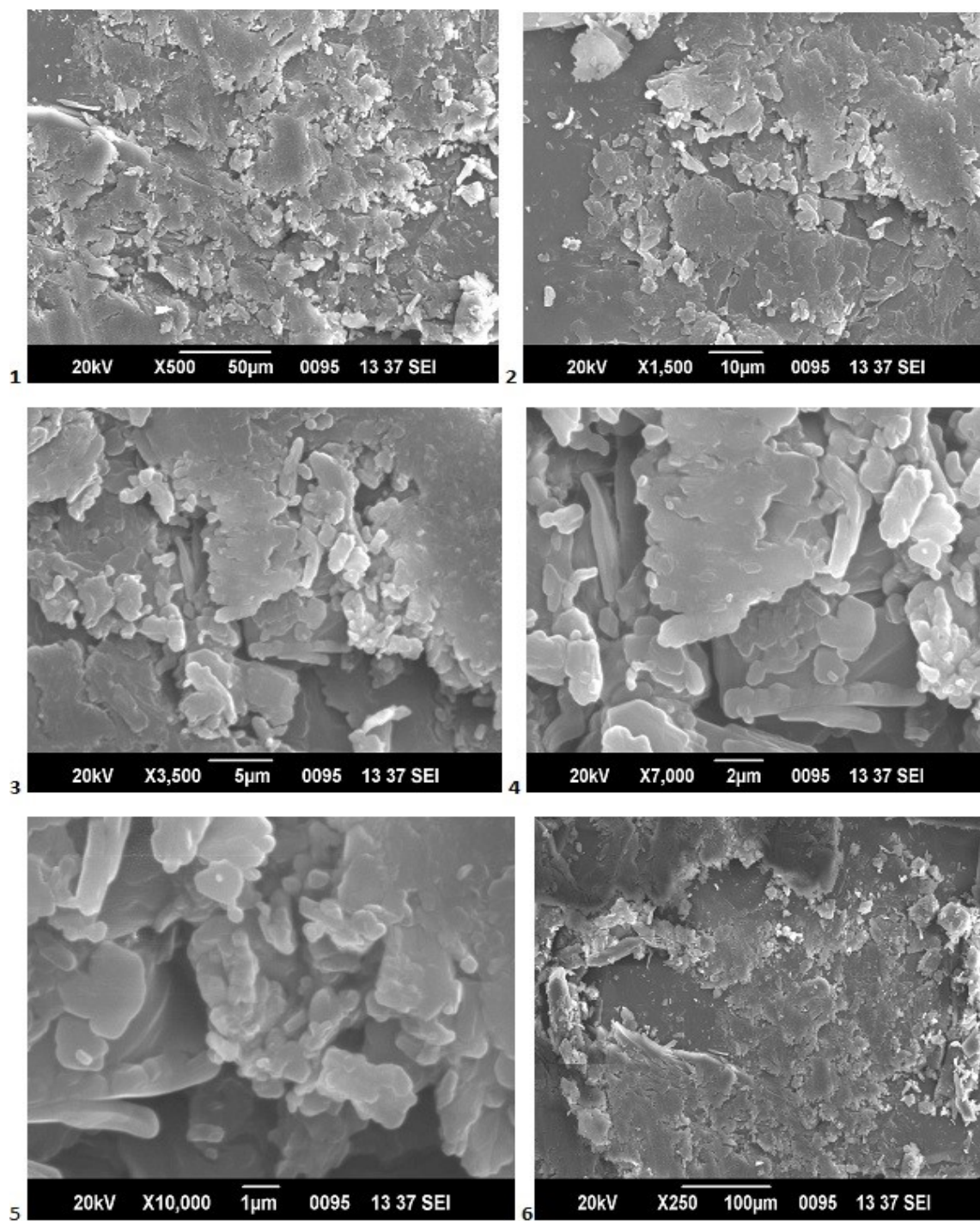


Fig.

S11. SEM micrographs (1-6) for H₂L^{SAL}.

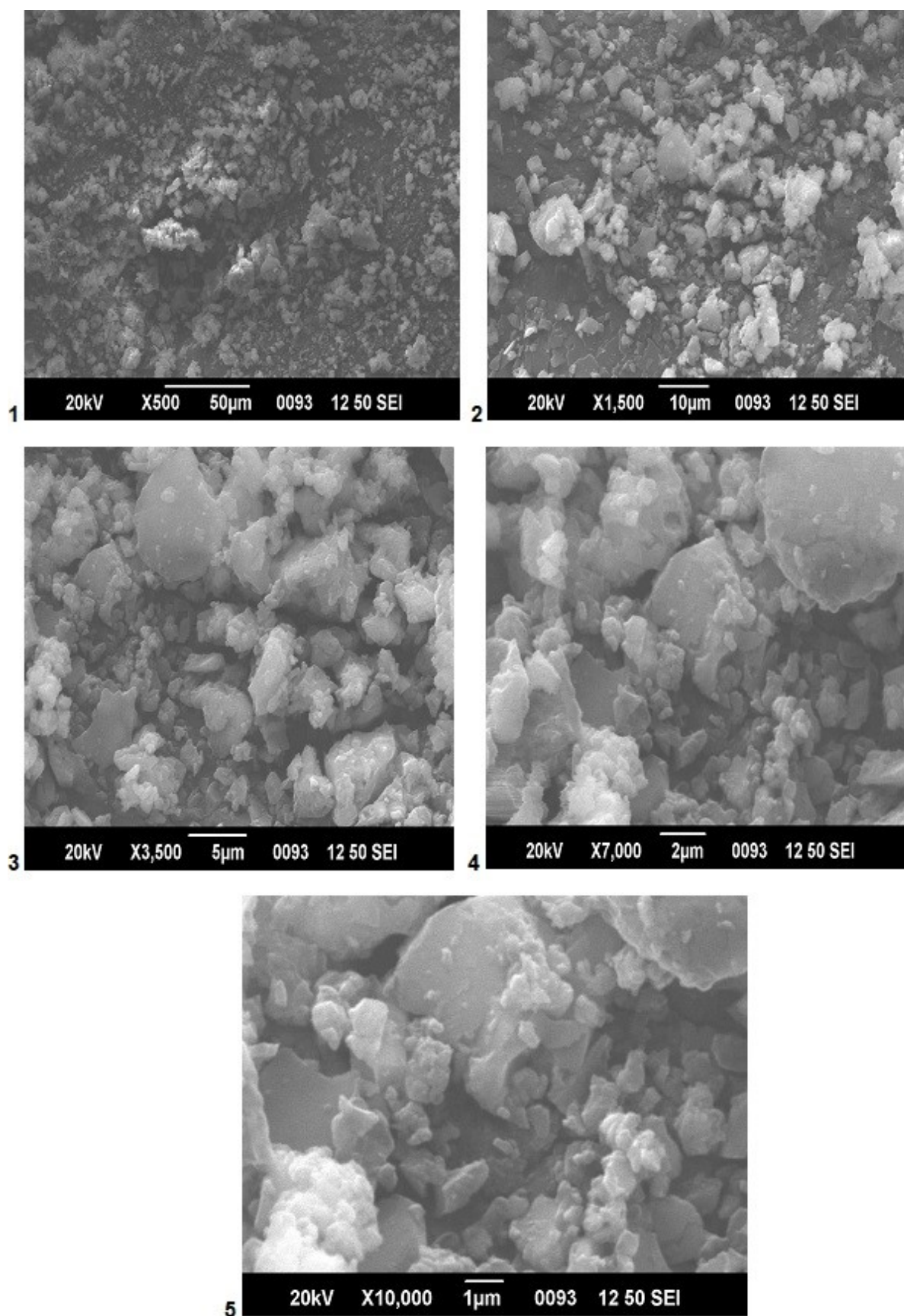


Fig.S12. SEM micrographs (1-5) for the copper complex.

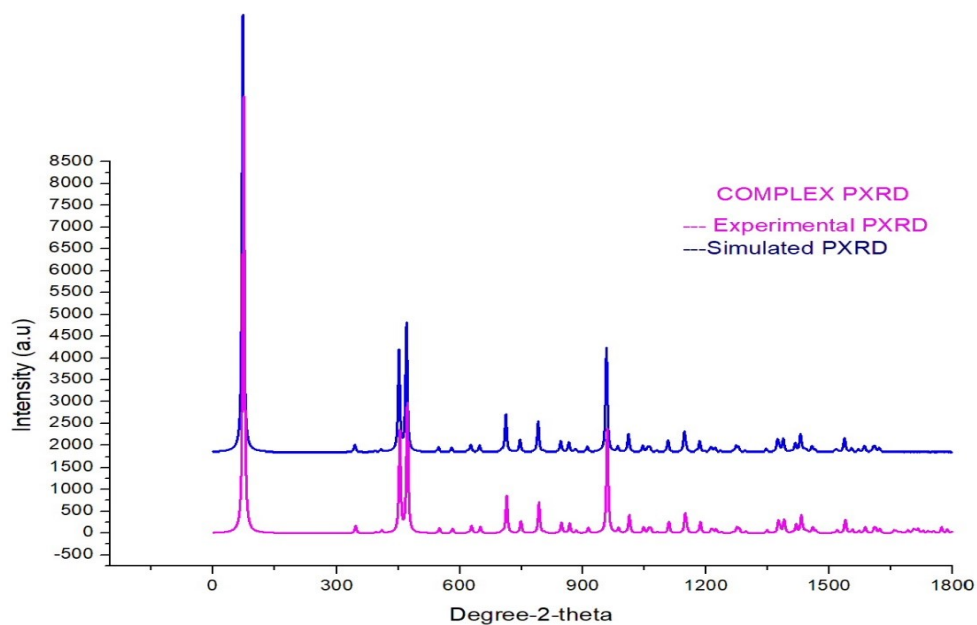


Fig.S13. Copper complex PXRD graph.

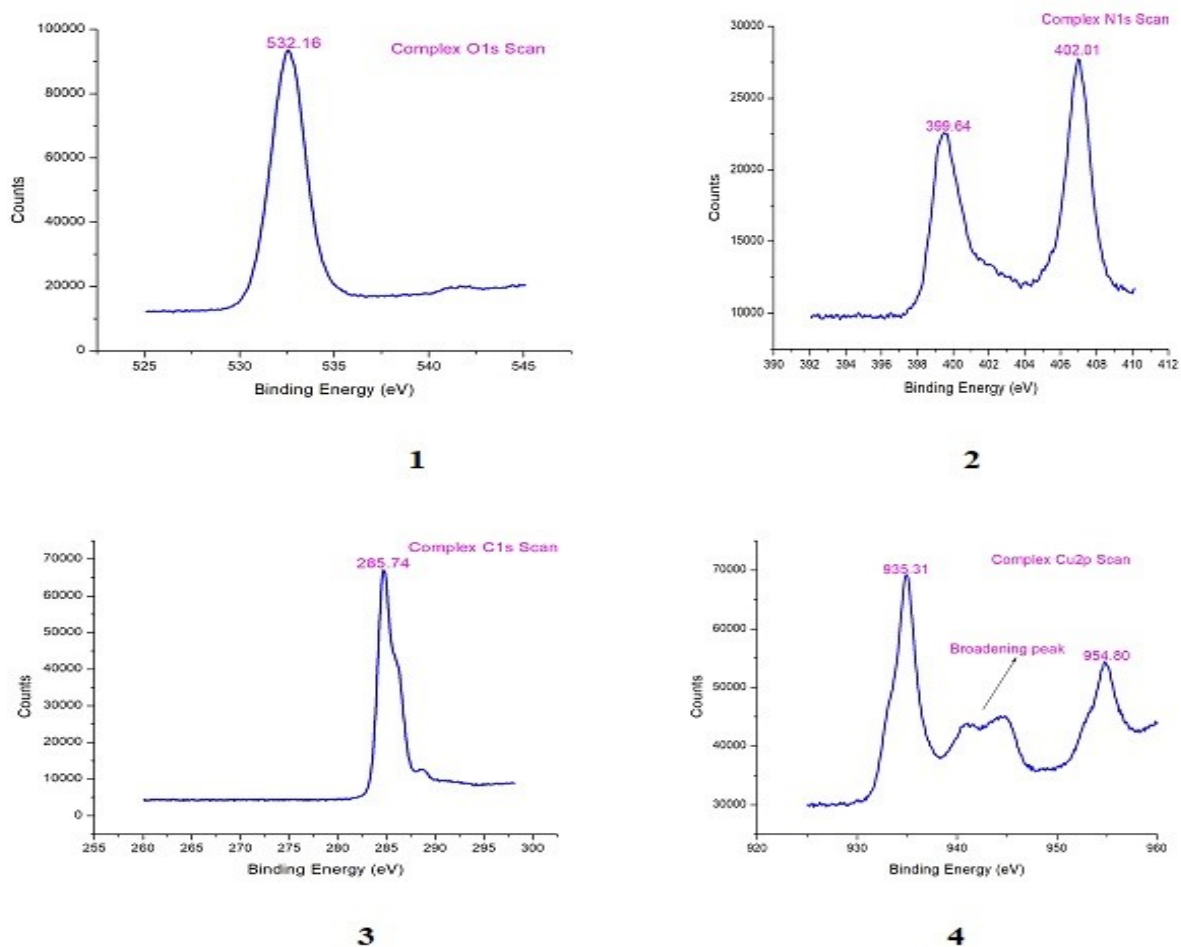


Fig.S14. XPS spectra of (1) O1s, (2) N1s, (3) C1s, and (4) Cu2p.

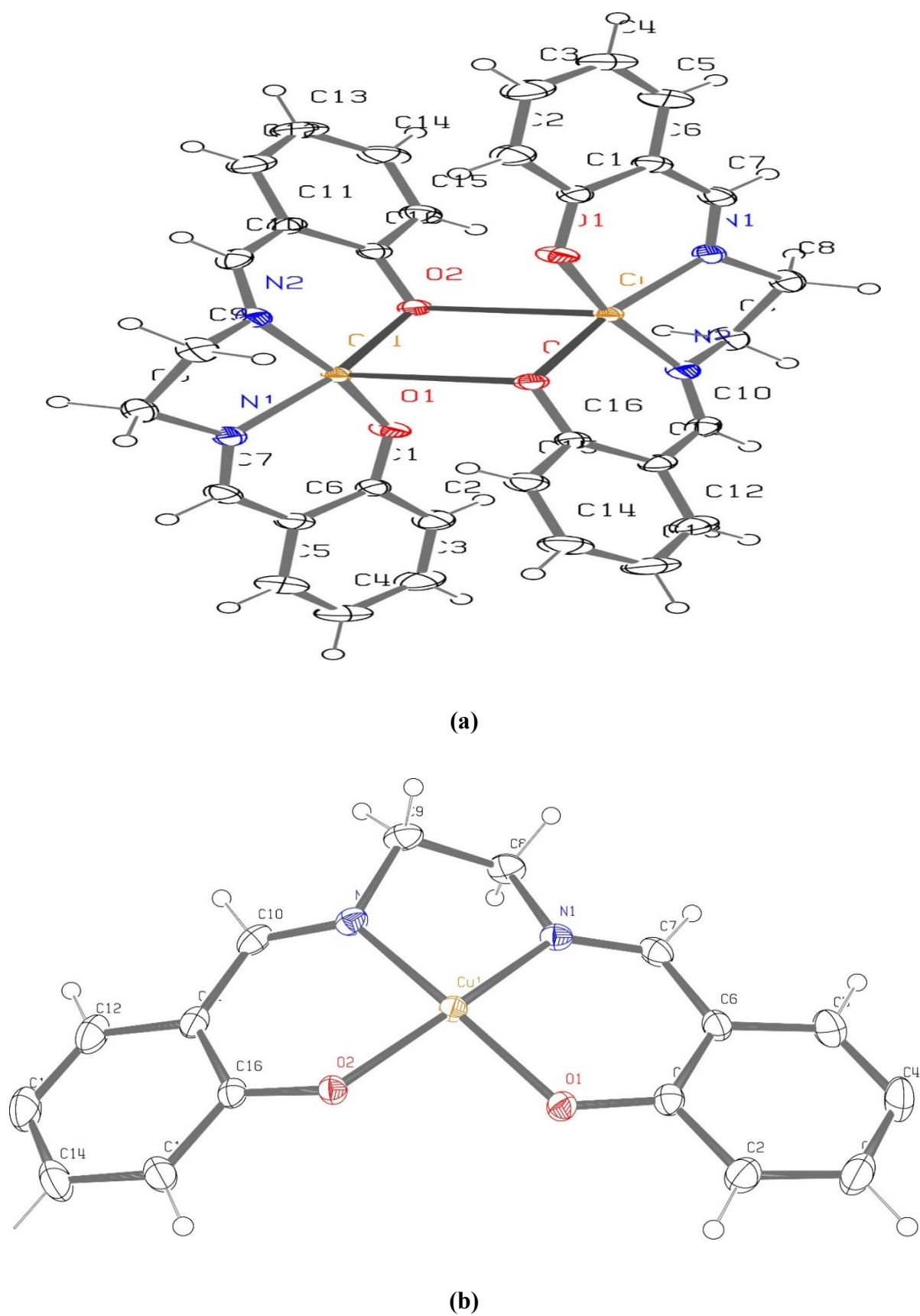


Fig.S15. ORTEP view of the complex (atoms are shown as 50% thermal ellipsoids).

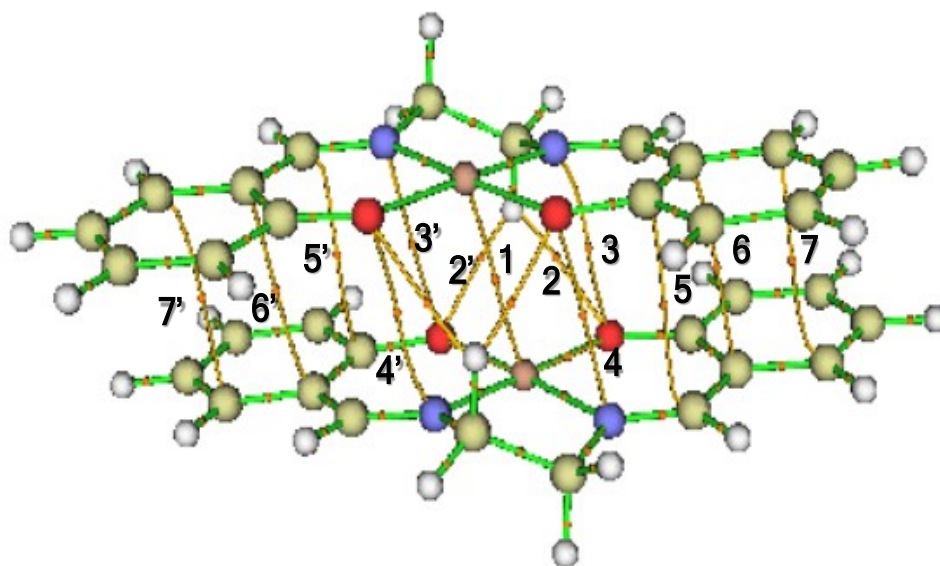


Fig.S16. QTAIM graph depicting BCPs of the studied complex.

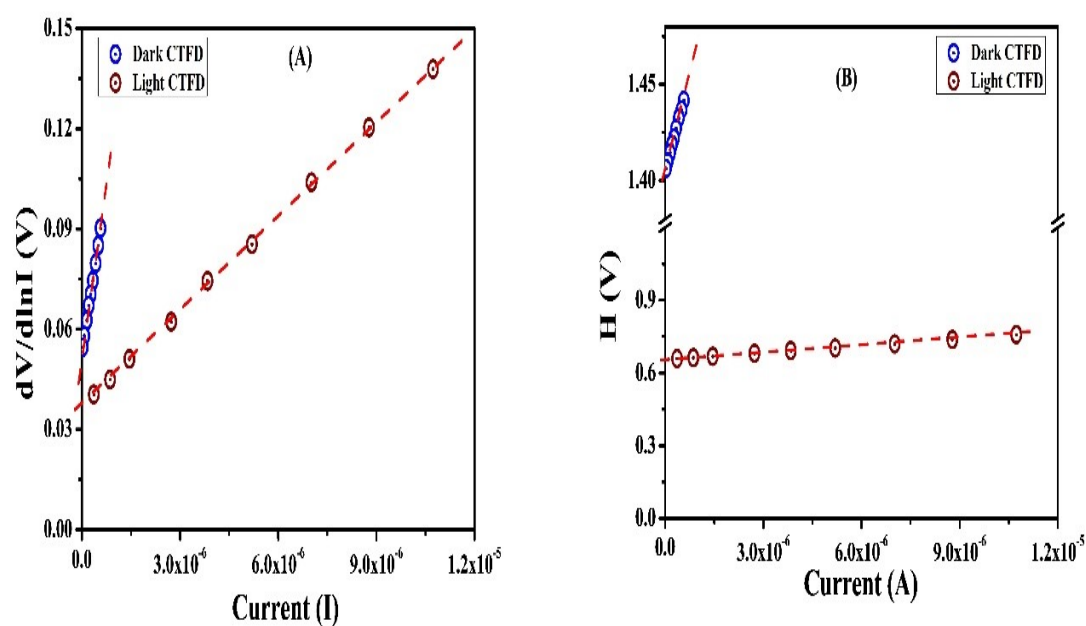


Fig.S17

(A) for $dV/d\ln I$ vs. I and S17(B) H vs. I curve for CTFD under dark and photo illumination conditions.

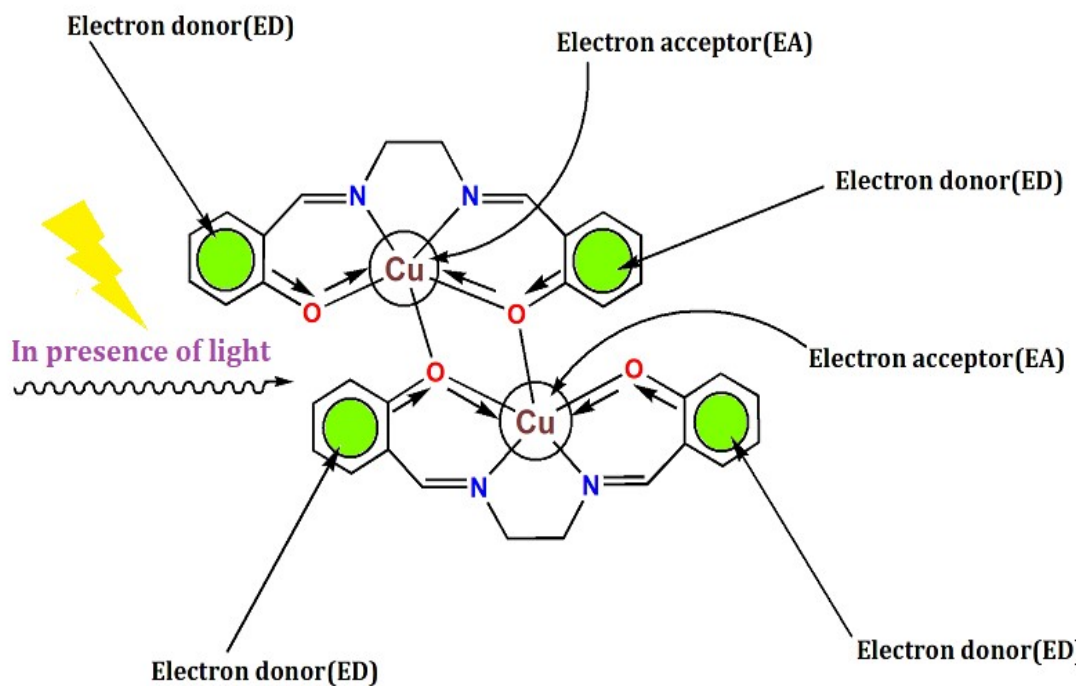


Fig.S18. A probable mechanism of photosensitivity of the copper complex.

References

1. M. Ghosh, S. Saha, A. Banerjee, D. Schollmeyer, A. Sarkar, and S. Banerjee, *New J. Chem.*, 2019, **43**, 16255-16263.
2. F. Ahmed, S. Halder, B. Dutta, S. Islam, C. Sen, S. Kundu, C. Sinha, P. P. Ray, and M. H. Mir, *New J. Chem*, 2017, **41**, 11317—11323.
3. B. Dutta, C. Sinha, and M. H. Mir, *J. Mol. Struct.*, 2019, **1197**, 430-435.
4. B. Dutta, A. Dey, K. Naskar, F. Ahmed, R. Purkait, S. Islam, S. Ghosh, C. R. Sinha, P. P. Ray, and M. H. Mir, *New J. Chem.*, 2018, **42**, 8629-8637.
5. B. Dutta, D. Das, K. Raksha, C. Sinha, S. Khanra, P. P. Ray, and M. H. Mir, *Mater. Adv.*, 2023, **4**, 215–222.
6. S. Khan, S. Halder, A. Dey, B. Dutta, P. P. Ray, and S. Chattopadhyaya, *New J. Chem.*, 2020, **44**, 11622-11630.

7. S. Khan, S. Halder, P. P. Ray, S. Herrero, R. González-Prieto, M. G. B. Drew, and S. Chattopadhyay, *Crystal Growth & Design*, 2018, **18**, 651-659.
8. M. Mondal, S. Jana, M. G. B. Drew, and A. Ghosh, *Polymer*, 2020, **204**, 122815
9. S. Halder, M. Das, K. Ghosh, A. Dey, B. B. Show, P. P. Ray, and P. Roy, *J Mater Sci.*, 2016, **51**, 9394–9403.
10. Ayub Tahmasbi 1, Akbar Jafari, and Abbas Nikoo, *Sci Rep.*, 2023, **13**, 10988.
11. S. Roy, A. Dey, P. P. Ray, J. Ortega-Castro, A. Frontera, and S. Chattopadhyay, *Chem. Commun.*, 2015, **51**, 12974–12976.
12. S. Halder, A. Layek, K. Ghosh, C. Rizzoli, P. P. Ray, and P. Roy, *Dalton Trans.*, 2015, **44**, 16149–16155.
13. S. Halder, A. Dey, A. Bhattacharjee, J. Ortega-Castro, A. Frontera, P. P. Ray, and P. Roy, *Dalton Trans.*, 2017, **46**, 11239–11249.
14. P. Ghorai, A. Dey, P. Brandaño, J. Ortega-Castro, A. Bauza, A. Frontera, P. P. Ray, and A. Saha, *Dalton Trans.*, 2017, **46**, 13531–13543.
15. S. Roy, S. Halder, M. G. B. Drew, P. P. Ray. and S. Chattopadhyay, *ACS Omega*, 2018, **3**, 12788–12796.
16. S. Khan, S. Halder, P. P. Ray, S. Herrero, R. González-Prieto, M. G. B. Drew, and S. Chattopadhyay, *Cryst. Growth Des.*, 2018, **18**, 651–659.
17. S. Konar, A. Dey, S. Ray Choudhury, K. Das, S. Chatterjee, P. P. Ray, J. Ortega-Castro, A. Frontera, and S. Mukhopadhyay, *J. Phys. Chem. C*, 2018, **122**, 8724–8734.
18. P. Ghorai, A. Dey, A. Hazra, B. Dutta, P. Brandaño, P. P. Ray, P. Banerjee, and A. Saha, *Cryst. Growth Des.*, 2019, **19**, 6431–6447.
19. S. Roy, A. Dey, M. G. B. Drew, P. P. Ray, and S. Chattopadhyay, *New J. Chem.*, 2019, **43**, 5020–5031.

20. S. Dey, S. Sil, B. Dutta, K. Naskar, S. Maity, P. P. Ray, and C. Sinha, *ACS Omega*, 2019, **4**, 19959–19968.
21. K. Ghosh, S. Sil, P. P. Ray, J. Ortega-Castro, A. Frontera, and S. Chattopadhyay, *RSC Adv.*, 2019, **9**, 34710–34719.
22. S. Roy, S. Halder, A. Dey, K. Harms, P. P. Ray, and S. Chattopadhyay, *New J. Chem.*, 2020, **44**, 1285–1293.
23. P. Ghorai, A. Dey, P. Brandaño, S. Benmansour, C. J. Go´mez Garcia, P. P. Ray, and A. Sahaw, *Inorg. Chem.*, 2020, **59**, 8749–8761.
24. S. Khan, S. Halder, A. Dey, B. Dutta, P. P. Ray, and S. Chattopadhyay, *New J. Chem.*, 2020, **44**, 11622–11630.
25. T. K. Ghosh, S. Jana, S. Jana, and A. Ghosh, *New J. Chem.*, 2020, **44**, 14733–14743.
26. A. Chandra, D. Das, J. O. Castro, K. Naskar, S. Jana, A. Frontera, P. P. Ray, and C. Sinha, *Inorg. Chim. Acta*, 2021, **518**, 120253.
27. S. Roy, A. Dey, R. M. Gomila, J. Ortega-Castro, A. Frontera, P. P. Ray, and S. Chattopadhyay, *Dalton Trans.*, 2022, **51**, 5721–5734.
28. S. Paul, B. Dutta, P. Das, S. Halder, M. Shit, P. P. Ray, K. Jana, and C. Sinha, *Appl. Organomet. Chem.*, 2023, **37**, e7160.
29. K. Debsharma, S. Dey, D. Das, S. Halder, J. Ortega-Castro, S. Sarkar, B. Dutta, S. Maity, K. Jana, A. Frontera, P. P. Ray, and C. Sinha, *CrystEngComm*, 2023, **25**, 162–172.
30. D. Majumdar, S. Roy, A. Dey and D. Sutradhar, *J. Mol. Struct.*, 2023, 1294, 136438.